This article has been accepted for inclusion in a future issue of this journal. Content is final as presented, with the exception of pagination.

Synthesis in Bandpass Domain of Star Junction Multiplexers With Acoustic Wave Ladder Filters

Mario Faura, *Graduate Student Member, IEEE*, Joel Mesas, *Graduate Student Member, IEEE*, Santi Cano, *Graduate Student Member, IEEE*, Laia Garcia, *Graduate Student Member, IEEE*, Jordi Verdú, *Senior Member, IEEE*, and Pedro de Paco, *Senior Member, IEEE*

***Abstract*—This work presents the first analytical method in the bandpass domain for the direct synthesis of multiplexers based on acoustic wave (AW) ladder filters connected in a star junction topology. The proposed method enables broadband modeling of multiport networks by computing the exact transfer function while accounting for the asymptotic behavior at both the origin and infinity, as well as controlling the frequency-dependent input and output (I/O) phases. Furthermore, by introducing a set of techniques to enhance numerical accuracy for polynomial evaluations and root-finding procedures, the new synthesis method is able to manage the high-order polynomials formulated in the real frequency domain. This methodology ensures the desired multiplexer response without channel loading degradation, allowing independent adjustment of return loss (RL) and transmission zeros (TZs) for each channel to fulfill the technological requirements of AW technology. The effectiveness and applicability of the proposed technique are rigorously demonstrated by means of two synthesized multiplexer examples, providing the Butterworth–Van Dyke (BVD) elements of each channel filter. This approach avoids intensive optimization procedures and represents a useful technique for the subsequent stages of AW filter design toward the final device layout.**

***Index Terms*—Acoustic wave (AW), bandpass domain, frequency denormalization error, ladder filter, multiplexer, narrowband approximation, reduced Chebyshev (RC) function, synthesis.**

I. Introduction

CARRIER aggregation (CA) schemes introduced in long term evolution (LTE) represent a key technique to increase usable bandwidth and thus achieve higher channel capacity. These CA approaches rely on the possibility of having multiple filters, one per each of the bands being aggregated, connected to the same antenna node [1], [2], [3]. Therefore, the challenge for acoustic wave (AW) technology is to provide multiplexer devices that implement several filters all sharing the same input port while maintaining the desired performance. However, the design of such a network has become a complex task due to the stringent requirements of isolation, rejection, and insertion loss to be fulfilled in multiple bands simultaneously [4]. Besides, the AW technology is highly restricted by some intrinsic constraints, such as the evenly distributed electromechanical coupling coefficient (k_t^2) for all the resonators or the minimum amount of external reactive elements [5], [6]. In this sense, synthesis techniques have proven essential in reducing optimization times by providing a quick starting point for the design of those AW filters that compose the multiplexer [7], [8].

In recent years, some contributions have been published on the synthesis and design of star junction AW multiplexers [9], [10], [11] and recently extended for manifold

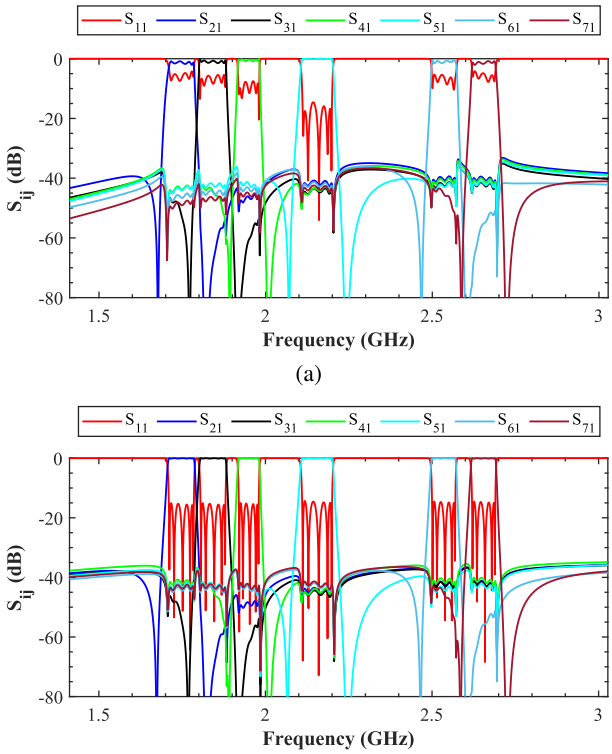

Fig. 1. Transfer function response of an LTE B3/B1/B7 hexaplexer synthesized using. (a) LP approximation from [9]. (b) Proposed DB approach.

Received 25 June 2026; revised 6 August 2026 and 3 September 2026; accepted 10 September 2026. This work was supported in part by the Agencia Estatal de Investigacion (AEI)–Ministerio de Ciencia e Innovación under Project PID2024-159605OB-I00 and in part by the Departament d'Universitats i Recerca. An earlier version of this paper was presented at the 2026 International Microwave Filter Workshop, Hong Kong, SAR China, February 7–9, 2026 [DOI: 10.1109/IMFW64610.2026.11419010]. *(Corresponding author: Mario Faura.)*

The authors are with the Department of Telecommunications and Systems Engineering, Universitat Autónoma de Barcelona, 08193 Barcelona, Spain (e-mail: marioesteban.faura@uab.cat).

Digital Object Identifier 10.1109/TMTT.2026.3734585

© 2026 The Authors. This work is licensed under a Creative Commons Attribution 4.0 License.
For more information, see https://creativecommons.org/licenses/by/4.0/

This article has been accepted for inclusion in a future issue of this journal. Content is final as presented, with the exception of pagination.

topologies [12]. Interestingly, while [9] proposed the first analytical method for the synthesis of multiplexers based on AW ladder filters connected in a star junction topology, [12] not only included the considerations inherent to herringbone or manifold configurations but also improved the numerical accuracy while maintaining fast execution times. Nevertheless, the increasing demand for wider bandwidth to be shared across multiple channels limits its multiplexer design process, since the narrowband technique, which makes use of the lowpass prototype (LP) approximation, leads to some degradation in the denormalized response. As depicted in the synthesized hexaplexer example of Fig. 1(a), if we use a large number of channels, the major contribution of error is shown in the outer bands matching with respect to the central frequency of the multiplexer bandwidth.

To address the frequency transformation errors, it has been observed that the major contribution comes from the input and output (I/O) elements of ladder networks, which primarily govern the asymptotic behavior at extreme frequencies. Aiming to escape from narrowband techniques, [13], [14], [15] have presented relevant contributions on direct bandpass (DB) synthesis, enabling accurate broadband modeling through an analytical computation of the transfer function directly in the bandpass domain while preserving the correct asymptotic behavior. It is worth noting that each DB methodology relies on a particular nodal representation of the ladder network, which consequently leads to different procedures for extracting the equivalent Butterworth–Van Dyke (BVD) elements. Nevertheless, these techniques are currently only available for standalone filters, so loading effects of adjacent channels are not considered. Moreover, the DB approach is heavily dependent on operations involving high-degree polynomials with clustered roots, which limits the maximum transfer function order that can be synthesized. Therefore, it is evident that enhancing numerical accuracy for polynomial evaluations and root-finding procedures [16], [17].

This work proposes a novel synthesis framework for multiplexers composed of AW ladder filters that overcomes the current limitations of narrowband techniques. In particular, the methodology is addressed for star junction multiplexers where all the AW filters begin with a series resonator. The proposed method is capable of computing the characteristic polynomials of the entire multiplexer in the bandpass domain through an iterative procedure. From the DB multiport function, the method derives a set of distorted polynomials for each channel filter such that, when connected at the star junction, they collectively implement an equiripple response. Once obtained, the synthesis of each ladder filter can be carried out separately. Thanks to the DB approach, the methodology enables a direct association between the characteristic polynomials of each channel and the real elements of the BVD circuit. As depicted in Fig. 1, this work ensures the exact solution for any fractional bandwidth (FBW). In addition, to mitigate round-off errors during synthesis procedures, this DB approach relies on accurate root-finding techniques rather than interpolated polynomial coefficients. This strategy takes advantage of the fact that the bandpass domain roots of each channel are already available once the filtering function is mapped from the LP domain to the bandpass domain. Since the logarithmic frequency mapping used in this article will cause small distortion, a slight modification of the filter functions is required to recover an equiripple response.

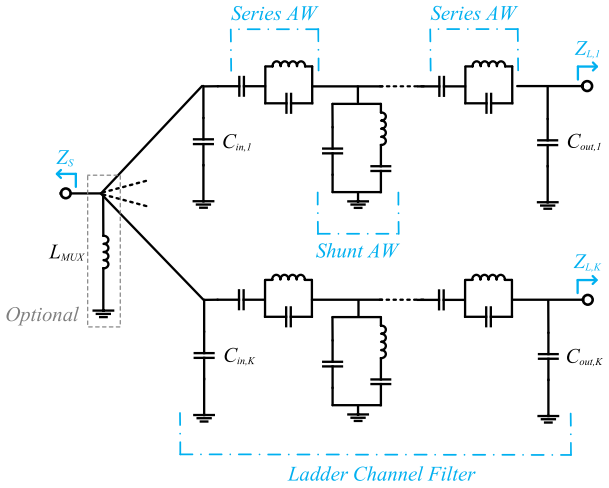

Fig. 2. Schematic view of the AW multiplexer proposed in this work: AW ladder filters connected to an ideal star junction. L_{MUX} is an optional input shunt inductor that can be considered during the synthesis process.

This article initially provides an overview of the proposed methodology and the mathematical formulation used to define the multiport characteristic polynomials, including the considerations inherent to AW multiplexers represented in the real frequency domain. While the recent conference publication in [18] focused on the general synthesis framework, the present article introduces the comprehensive synthesis steps, starting from an equiripple Chebyshev response for each channel and then covering how to derive the new set of channel polynomials from their multiport counterparts. To validate the proposed method, two synthesis examples are presented: the first example provides a clear illustration of the methodology, whereas the second example highlights the practical use of the method in providing an excellent starting point for the AW multiplexer design.

II. Definitions of Star Junction AW Multiplexers in Bandpass Domain

Commonly, AW multiplexers are implemented using a star junction model where all the channels are directly connected to a common node. Each ladder filter is composed of AW resonators disposed in alternating series and shunt positions and implements filter responses of order N, where N is the number of AW resonators. The overall reactance model of the star junction multiplexer is shown in Fig. 2, where for this work it is assumed that each channel filter starts in a series resonator. This is a modeling choice rather than a fundamental limitation, since the method can be equally applied to shunt-starting channels by consistently redefining the bandpass filtering function and the multiport polynomial derivation.

Regarding the I/O capacitors, they are required to prepare the extraction of the first and last resonators. Under these assumptions, a single capacitive element shunted to ground (C_{MUX}) can be simplified by merging the input capacitors of

This article has been accepted for inclusion in a future issue of this journal. Content is final as presented, with the exception of pagination.

each filter. It is worth noting that, in practical implementations, this capacitor is frequently omitted and replaced with an optimized inductor that provides an approximation [1]. In many cases, to achieve the desired matching between filters, multiple reactive elements are needed acting as matching networks to compensate for the total reactance at the junction [19]. However, following the method in this work, the multiplexer can be analytically synthesized to implement an ideal star junction without the need for any extra matching elements. Furthermore, it must be mentioned that the presented methodology can include the presence of a common node inductance (denoted as L_{MUX}) as a degree of freedom in the search for technology feasibility.

A. Filtering Function of Series-Starting Ladder Network

Having presented the details of the multiplexer configuration, the first step of any synthesis methodology is modeling the transfer function to realize in terms of rational polynomial functions. The response of an Nth order AW ladder filter is modeled in the normalized frequency domain $s = \Sigma + j\Omega$ with the characteristic polynomials $F(s)$, $P(s)$, and $E(s)$ that define the S-parameters as

$$S_{11}(s) = \frac{F(s)/\varepsilon_r}{E(s)} \quad S_{21}(s) = \frac{P(s)/\varepsilon}{E(s)} \tag{1}$$

where ε_r and ε are the normalization constants that ensure monic polynomials. The roots of $P(s)$, $F(s)$ and $E(s)$ represent the transmission zeros (TZs), reflection zeros (RZs) and poles of the ladder topology, respectively. Taking into account the LP approximation, the filter passband is defined in the $s = [-j, j]$ interval, and the polynomials, considering a fully canonical generalized Chebyshev (GC) filter function, are computed following the procedure in [20].

Going back to the series-starting case of Fig. 2, one TZ is controlled by the series capacitors at $\Omega = 0$ (an additional zero appears if L_{MUX} is considered), while another zero is controlled by the shunt capacitors at $\Omega = \infty$. Nevertheless, the vertical asymptotes that appear when the ladder circuit is evaluated at the extreme frequencies are neglected in the LP domain because BVD resonators and I/O elements are partially and fully modeled, respectively, by frequency-invariant reactances (FIRs), which do not account for frequency-dependent slopes [21]. Therefore, when these FIRs are scaled via the bilateral transformation, uncontrolled asymptotes appear at extreme frequencies, ultimately degrading the in-band response as the FBW increases.

The DB response must explicitly account for the missing TZ at the origin and infinity, and control the out-of-band (OoB) fly backs by adding complex/real RZs. In this scenario, the filtering function is no longer fully canonical because now the k-channel order is $N_k^{DB} = 2N_k + 2$ and the number of finite TZs is $n_{tz,k}^{DB} = 2N_k + 1$, where N_k is the number of filter resonators of the k-channel. Furthermore, each k-channel reflection polynomial $F_k(s)$ must include a phase shift of 180° due to the nature of the network, as depicted in Fig. 2 (i.e., $\varepsilon_{r,k} = -1$). On the one hand, Fig. 3(a) shows the DB root pattern of an arbitrary $F_k(s)$. Notice that $2N_k$ roots lie on the imaginary axis and model the positive and negative parts of the spectrum, while the pair of real RZs allow to manage the I/O phases. On the other hand, the roots of an arbitrary k-channel transmission polynomial $P_k(s)$ are depicted in Fig. 3(b), where one TZ is located at the origin.

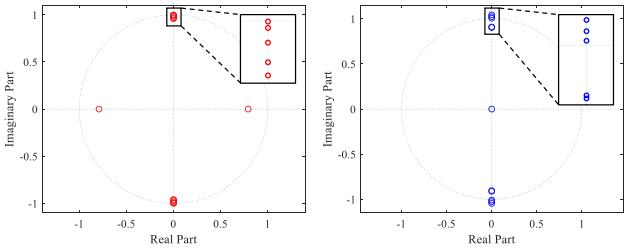

(a) (b)

Fig. 3. Definition of the standalone ladder filtering function in the DB domain: root pattern of (a) polynomial $F(s)$ and (b) polynomial $P(s)$.

B. Derivation of DB Multiport Polynomials

The polynomial characterization of a star junction AW multiplexer in the bandpass domain departs from the narrowband approaches described in [9] and [22]. The S-parameters of a multiport network are expressed as follows:

$$S_{11}(s) = \frac{u_0 U(s)}{D(s)}, \quad S_{k+1,1}(s) = \frac{t_k T_k(s)}{D(s)} \tag{2}$$

where $U(s)$, $D(s)$, and $T_k(s)$ are monic polynomials while u_0 and t_k are normalization constants. It should be noted that channel isolation is not explicitly parametrized, but is implicitly determined by the individual OoB rejection of each channel. Nevertheless, this assumption may not be valid for contiguous channels.

Computing equiripple multiplexer polynomials entails an iterative procedure that originally assumes equiripple Chebyshev polynomials at each channel, namely $P_k^{(0)}(s)$, $F_k^{(0)}(s)$, $E_k^{(0)}(s)$, $\varepsilon_k^{(0)}$, and $\varepsilon_{r,k}^{(0)}$. Since the methodology is leveraged in a DB synthesis approach, it will be required to build a dual-band filter function, symmetric with respect to zero frequency, to capture the bandpass asymptotic behavior in the normalized domain. These kinds of filtering responses can be computed using a Remez-like algorithm [23], but this technique shows some numerical limitations for the DB compressed domain. Instead, the initial polynomials are built through an intermediate reduced Chebyshev (RC) response by adding an additional complex RZ in the LP domain, which is then transformed to the DB domain using a mapping function [13].

The objective of the iterative method is to find the set of multiport polynomials that describe an ideal multiplexer response whose common port return loss (RL) (CPRL) is equiripple within each channel band. From the computed multiport polynomials, a new set of distorted channel polynomials and normalization constants can be derived. These new polynomials do not exhibit a perfect equiripple response anymore if evaluated as a standalone filter. They incorporate a deliberate distortion in the location of roots such that they are ready to be connected along with the partner filters in the multiplexer. A conceptual map of this process is depicted in Fig. 4. This final set of distorted polynomials allows us to

This article has been accepted for inclusion in a future issue of this journal. Content is final as presented, with the exception of pagination.

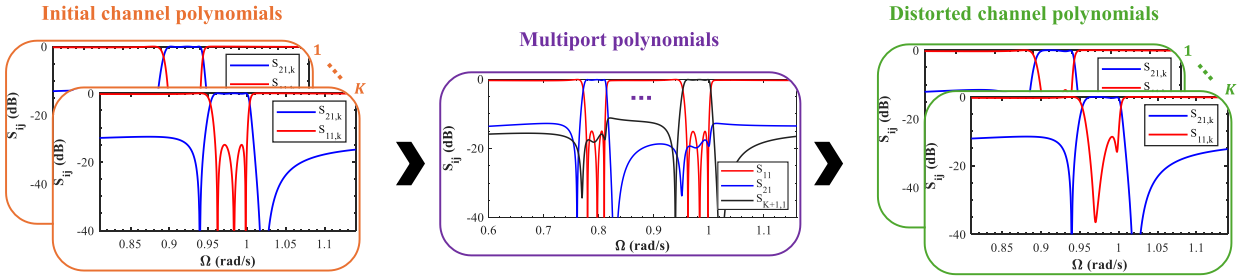

Fig. 4. Graphical abstract of the polynomial computation procedure within the DB multiplexer synthesis framework. From a Chebyshev seed per channel, multiport equiripple polynomials are obtained. From the resulting multiport function, a set of distorted channel polynomials are derived and independently synthesized. Notice that a zoom of the positive spectral duality to better visualize the in-band transfer function behavior.

independently synthesize each of the channel filters following the procedure in [13].

Let us start by defining the relationships between the channel polynomials and the joint multiport response polynomials. Consider topology in Fig. 2 and assume that $F_k(s)$ and $E_k(s)$ are known. Therefore, the input admittance formulation of each individual channel $y_{in,k}$ can be expressed as

$$y_{in,k} = \frac{E_k(s) - f_k F_k(s)}{E_k(s) + f_k F_k(s)} = \frac{E_k(s) + F_k(s)}{E_k(s) - F_k(s)} = g_k \frac{D_k(s)}{S_k(s)} \tag{3}$$

being

$$\begin{aligned} D_k(s) &= \frac{E_k(s) + F_k(s)}{2} \\ S_k &= \frac{E_k(s) - F_k(s)}{cS_{1,k}} \\ g_k &= \frac{2}{cS_{1,k}} \end{aligned} \tag{4}$$

where $cS_{1,k}$ is the leading coefficient of S_k and f_k is the normalization constant of the polynomial F_k defined as $f_k = 1/\varepsilon_{rk}$.

For star junction multiplexers, the common port input admittance is always equal to the sum of all channels' $y_{in,k}$. Under this condition and considering the definition of reflection parameter S_{11} from input admittance, $U(s)$ and $D(s)$ can be derived as follows:

$$U(s) = S(s) - \sum_{k=1}^{K} g_k D_k(s) W_k(s) \tag{5}$$

$$D(s) = S(s) + \sum_{k=1}^{K} g_k D_k(s) W_k(s) \tag{6}$$

being

$$W_k(s) = \prod_{i=1, i\neq k}^{K} S_i(s) \qquad S(s) = \prod_{k=1}^{K} S_k(s). \tag{7}$$

If a junction admittance equal to $1/sL_{MUX}$ is considered at multiplexer common port, the definitions of $U(s)$ and $D(s)$ are slightly changed

$$U(s) = sL_{MUX}S(s) - S(s) - sL_{MUX}\sum_{k=1}^{K} g_k D_k(s) W_k(s) \tag{8}$$

$$D(s) = sL_{MUX}S(s) + S(s) + sL_{MUX}\sum_{k=1}^{K} g_k D_k(s) W_k(s). \tag{9}$$

Applying the same reasoning as before to the transmission term (i.e., $S_{k+1,1}$), it can be demonstrated that $T_k(s) = P_k(s)W_k(s)$. Furthermore, it can be stated that $u_0 = -1$ and coefficients t_k are given by

$$t_k = \frac{p_k g_k}{G} \tag{10}$$

where term $p_k = 1/\varepsilon_k$ is the normalization constant and $G = \sum_{k=1}^{K} g_k$.

III. General Synthesis Methodology

A. DB Mapping of Chebyshev Channels

If an LP approximation is considered, the polynomial definitions in (2) define K passbands within the original $s = [-j, j]$, each located in its corresponding position such that their equivalence in the bandpass domain is given by $s = -j \rightarrow f = f_L$ and $s = j \rightarrow f = f_U$, where f_L denotes the lower passband limit of the first channel and f_H denotes the upper passband limit of the last channel. On the contrary, the DB domain modifies the LP response through an intermediate step by introducing a complex RZ that models the I/O phases using RC functions [24]. With this approach, the filtering function is no longer fully canonical, and the position of the complex RZ will affect the OoB flybacks. Subsequently, an additional TZ at zero frequency is introduced to fully define the ladder transfer function by mapping all zeros and poles of the LP response into the real domain using a logarithmic mapping function adopted from [25], which preserves the same information in both the positive and negative frequency planes. As a result, the new passband becomes symmetric around 0, although it may remain asymmetric with respect to the center frequency.

To obtain the roots of polynomials $F(s)$ and $P(s)$ in the DB domain, as shown in Fig. 3(a) and (b), respectively, a logarithmic mapping function is used, increasing the order of the k-channel to $N_k^{DB} = 2N_k + 2$ with one TZ at the origin. Under this decision, the mapping function has been uniquely defined in the Ω-plane as follows:

$$\begin{cases} \Omega = 1 + \eta \log_{10}\left(-\Omega'\right), & \text{if} \quad \Omega' < 0 \\ \Omega = 1 + \eta \log_{10}\left(\Omega'\right), & \text{if} \quad \Omega' > 0 \end{cases} \qquad \eta = \frac{2}{\log_{10}(f_2/f_1)} \tag{11}$$

where f_1 and f_2 are the lower and higher corner frequencies, Ω is the frequency variable in the single-band domain, and Ω'

This article has been accepted for inclusion in a future issue of this journal. Content is final as presented, with the exception of pagination.

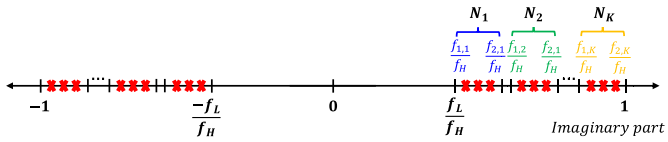

Fig. 5. Imaginary parts distribution of RZs in the DB domain.

is the frequency variable in the dual-band domain, in such a way that $\Omega(\Omega') = \pm 1$, for $\Omega' = [-1, -f_1/f_2, f_1/f_2, 1]$.

Nevertheless, this mapping is only valid for standalone filters and cannot represent the overall multiplexer response of K channels in the real frequency domain. Therefore, the dual-band channel polynomials need to be linearly mapped to their respective position within the frequency range $\Omega'' = [-1, -f_L/f_H, f_L/f_H, 1]$, considering each channel's passband limits. As a result, each function is compressed into the DB multiport domain, and the initial roots of $P_k^{(0)}(s)$, $F_k^{(0)}(s)$, and $E_k^{(0)}(s)$ are obtained, providing the starting point for the iterative procedure. As an illustrative example, Fig. 5 shows the imaginary part distribution of RZs after applying the DB mapping.

B. Iterative Procedure of Multiport Polynomials

The target response is a CPRL that is as equiripple as possible within the passband of each channel to obtain the highest OoB isolation and best passband ripple. As discussed in [22], the monic version of $U(s)$ can be obtained from the roots of the initial $F_k^{(0)}(s)$ to achieve a practically equiripple solution. Notice that in DB synthesis, the positive real RZ corresponds to the input capacitor of each independent standalone channel. However, since the multiplexer network contains a merged capacitor at the common port, only one of the K initial positive real RZs must be considered in the reflection polynomial. Therefore, it can be stated that $U(s)$ and $D(s)$ are polynomials of degree $M = \sum_{k=1}^{K} N_k^{DB} - K + 1$, and $T_k(s)$ of degree $M-1$. Interestingly, common port shunt inductors contribute an extra TZ at the origin in $T_k(s)$ and replace the single positive real RZ with a positive pair of conjugated RZs in $U(s)$.

Having the M roots of $U(s)$ defined, the iterative procedure starts by computing the first iteration of the intermediate polynomial $S(s)$, which contains $S_k(s)$ subpolynomials obtained from (4)

$$S^{(0)}(s) = \prod_{k=1}^{K} S_k^{(0)}(s) = \prod_{k=1}^{K} \frac{E_k^0(s) - F_k^0(s)}{cS_{1,k}^0} \tag{12}$$

where $cS_{1,k}^{(0)}$ is equal to $\sum_{i=1}^{N_k^{DB}} zF_{k,i}^{(0)} - \sum_{i=1}^{N_k^{DB}} zE_{k,i}^{(0)}$, being $zF_{k,i}^{(0)}$ and $zE_{k,i}^{0}$ the roots of $F_k^{(0)}(s)$ and $E_k^{(0)}(s)$, respectively.

After that, considering the $T_k(s)$ definition, the desired value of RL must be imposed at one corner frequency per channel, denoted as $\Omega_{c,k}$. Applying the unitary conditions, coefficients t_k can be obtained isolating the next equation related to the S_{11} definition

$$\frac{\left|U\left(j\Omega_{c,k}\right)\right|^2}{\left|U\left(j\Omega_{c,k}\right)\right|^2 + \sum_{k=1}^{K} |t_k|^2 \left|T_k^{(0)}\left(j\Omega_{c,k}\right)\right|^2} = 10^{-\frac{RL_k}{10}}. \tag{13}$$

At this point, $U(s)$, $T_k^{(0)}(s)$ and coefficients $t_k^{(0)}$ are known. By revisiting the Feldtkeller equation (FE), a pseudodenominator polynomial $D(s)^2$ can be expressed as

$$D(s)\,D^*(-s) = U(s)\,U^*(-s) + \sum_{k=1}^{K} |t_k|^2\; T_k(s)\,T_k^*(-s). \tag{14}$$

Notice that the $2M$ roots of the polynomial $D(s)^2$ are known, and $D^{(0)}(s)$ can be found by taking only those roots whose real part lies in the left-half-plane of s (Hurwitz stability criterion). Following all the previous steps, up to this point the procedure has made the zeroth iteration of the multiport polynomial synthesis. Nevertheless, observe that a new version of $S(s)$ can be computed from a given pair of $D(s)$ and $U(s)$

$$\delta_1 S(s) = \frac{\sum_{k=1}^{K} g_k \left(D(s) - U(s)\right)}{2} \tag{15}$$

where δ_1 represents the highest degree coefficient of $D(s) - U(s)$ and can be computed from $\sum_{n=1}^{M} zU_n - \sum_{n=1}^{M} zD_n$, being zU_n and zD_n the roots of $U(s)$ and $D(s)$, respectively. Furthermore, if L_{MUX} is considered in the multiplexer network, an additional pole will appear at zero frequency after applying the subtraction of the previous polynomials. Note that this root must be removed when recovering the channels' input admittance poles to avoid breaking the convergence of the method.

Notice that (15) leads to the computation of a new estimation of polynomial $S(s)$, let this be $S^{(m+1)}(s)$, which plainly differs from the initial guess $S^{(0)}(s)$. However, the same method can be applied to compute the next iteration of the multiport polynomials [i.e., $t_k^{(m+1)}$, $T_k^{(m+1)}(s)$, and $D^{(m+1)}(s)$] until the roots of $S^{(m+1)}(s)$ converge to a predefined level compared to $S^{(m)}(s)$, resulting in a sufficiently stable solution. Ideally, final $S(s)$ should be a monic polynomial (i.e., $\delta_1 = 1$), so also coefficients g_k must be updated as $g_k^{(m+1)} = g_k^{(m)}/\delta_1^{(m+1)}$ to achieve this criteria of convergence.

C. Equlization of Common Port RL Equiripple

This section illustrates the proposed additional synthesis step which is tailored to equalize the CPRL equiripple. Following the same strategy as in [26], the location of the purely imaginary RZs is adjusted along the imaginary axis in an analytical and controlled manner according to the desired characteristic function. By definition, the characteristic function $C(\Omega)$ describes the ripple of the passband. When the filter is equiripple, $C(\Omega)$ oscillates with a constant amplitude $|\Delta|$ across the passband. For multiplexer networks, the characteristic function can be expressed as

$$C_k(\Omega) = \frac{U(\Omega)}{T_k(\Omega)}. \tag{16}$$

As depicted in Fig. 6(a), within the positive k-passband of the DB domain (for duality, the same occurs in the negative part of the spectrum), there is a set of frequency points where $|C_k(\Omega)|$ achieves maximum values, commonly referred to as extrema points and denoted as $\Omega_{k,i}$. The $N_k + 1$ extrema points can be obtained using the derivative of the characteristic function of expression (16). Nonetheless, this step is heavily

This article has been accepted for inclusion in a future issue of this journal. Content is final as presented, with the exception of pagination.

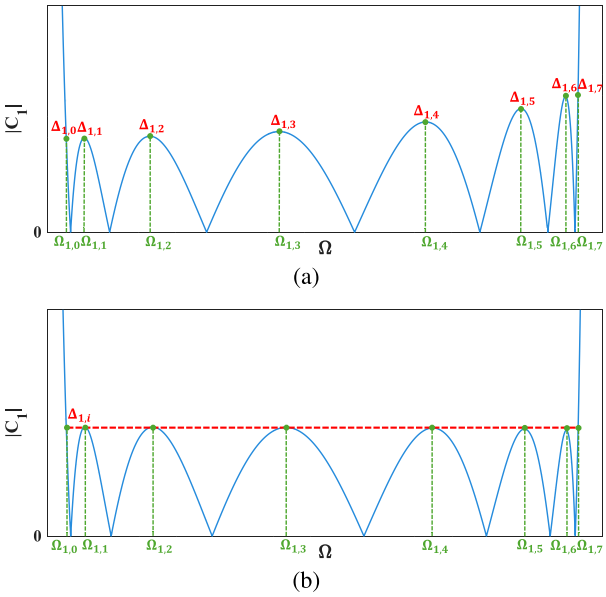

Fig. 6. In-band characteristic function of the first transmission channel (positive Ω values). (a) $|C_1|$ without correction. (b) $|C_1|$ with equalization.

dependent on operations involving high-degree polynomials, which can lead to numerical issues. A more numerically stable approach, and really close to the mathematical definition, is proposed in this work

$$\left.\frac{\partial C_k(\Omega)}{\partial \Omega}\right|_{\Omega\in[\Omega_{k,0},\Omega_{k,N_k}]} \simeq \frac{\partial\left(F_k^{(0)}(\Omega)/P_k^{(0)}(\Omega)\right)}{\partial\Omega} = 0 \qquad (17)$$

where $\Omega_{k,i}$ can be located by finding the maximum of $|U(\Omega)/T_k(\Omega)|$ within the interval $[\Omega_{k,i}, \Omega_{k,i+1}]$.

Indeed, the in-band ripple can be modified using a set of real scaling factors $\alpha_{k,i}$ responsible to modify the characteristic function just at the extrema points. Therefore, the factor $\alpha_{k,i}$ necessary to compensate the equiripple deviation shown in Fig. 6(a) can be found by evaluating the characteristic function at $\Omega_{k,i}$ and knowing that RL_k value is forced at $\Omega_{c,k}$

$$\left|C_k\left(\Omega_{k,i}\right)\right| = \left|\frac{U\left(\Omega_{k,i}\right)}{T_k\left(\Omega_{k,i}\right)}\right| = \left|\Delta_{k,i}\right| \qquad (18)$$

and consequently

$$\alpha_{k,i} = \frac{\left|C_k\left(\Omega_{c,k}\right)\right|}{\left|\Delta_{k,i}\right|}. \qquad (19)$$

Having the extrema points and the scaling factors, a set of linear equations for each channel must be solved to update the reflection polynomial. Therefore, by exploiting the approach in (17) and expressing the required $F_k(\Omega)$ evaluated for all $\Omega_{k,i}$ as a function of their unknown coefficients, the problem can be simplified in matrix notation terms as $\mathbf{A}\cdot\mathbf{x} = \mathbf{b}$. Then, $\mathbf{x}$ must be isolated considering the following definitions where the k subscript notation has been dropped for simplicity:

$$\begin{aligned}\mathbf{x} &= \left[f_{N-1}, f_{N-2}, \ldots, f_0, \Delta\right]^T\\ \mathbf{b} &= \left[-\Omega_1^N, -\Omega_2^N, \ldots, -\Omega_{N+1}^N\right]^T\\ \mathbf{A} &= \left[\Omega_i^{N-1}, \Omega_i^{N-2}, \ldots, 1, (-1)^{i-1}\,\alpha_i P(\Omega_i)\right]\end{aligned} \qquad (20)$$

where $\mathbf{x}$ is composed of the N unknown coefficients f_n and the amplitude Δ. Moreover, matrix $\mathbf{A}$ includes the set of α_i in its last column and alternates the signs between consecutive indices i.

Once the last matrix equation is solved, the next step is to update the frequency sample points Ω_i by applying (17) with the new values of $F(\Omega)$. Following the principle of the Remez algorithm, the last two steps are repeated until convergence. Furthermore, notice that the positive roots of dual-band polynomials $F(\Omega)$ and $P(\Omega)$ may be temporarily returned to the original single-band domain of each channel polynomial to keep the numerical accuracy. It should be noted that iteratively modifying the polynomial $U(s)$ may compromise the convergence of the synthesis procedure. Therefore, this strategy consists of applying the proposed method only after the first iteration, once $T_k(s)$ is updated, as this is the critical synthesis stage where $S^{(m+1)}(s)$ and $S^{(m)}(s)$ differ the most. Consequently, Fig. 6(b) demonstrates that, at the end of the synthesis procedure, the in-band characteristic function of each channel evaluated at any extrema point is practically coincident with a constant amplitude (i.e., the CPRL equiripple will be equalized).

D. Derivation of Distorted Channel Polynomials

Knowing the multiport polynomials $U(s)t_kT_k(s)$ and $D(s)$, the objective is to split the multiplexer response into the distorted channel polynomials that compose it. Notice that all g_k and $S_k(s)$ are already known (output of the iterative procedure). Therefore, the objective is finding subpolynomials $D_k(s)$ to retrieve the channel polynomials from (4). From its definition, $D_k(s)$ is a monic polynomial of degree N_k^{DB} with one root at zero frequency. Therefore, among its $N_k^{DB}+1$ coefficients, only $N_k^{DB}-1$ are unknown. Determining these coefficients requires $N_k^{DB}-1$ points at which the value of $D_k(s)$ is known, allowing polynomial interpolation. For this purpose, let us define the following for the kth channel:

$$D'_k(s) = \frac{D_k(s)}{s} - s^{N_k^{DB}-1}. \qquad (21)$$

Bringing (21) into (6) or (9) and evaluating either of both resulting equations at S_k roots, namely zS_k, would yield

$$D'_k(zS_k) = \frac{G\,D(zS_k)}{C g_k W_k(zS_k)} - zS_k^{N_k^{DB}-1} \qquad (22)$$

where the constant C can be equal to zS_k (junction without L_{MUX}) or zS_k^2 (junction with L_{MUX}).

To find $D'_k(s)$ coefficients, the $N_k^{DB}-1$ linear system of equations can be solved through a Vandermonde matrix as introduced in [22]. However, the interpolation method described in [22] has numerical limitations when applied to the DB approach due to the high-order polynomials. In that sense, this article proposes in Section IV-C to enhance the numerical accuracy by computing the roots of $D_k(s)$ through a modified Newton–Raphson (NR) method.

Having obtained $D_k(s)$, the next step is to derive the distorted channel polynomials $F_k(s)$ and $E_k(s)$ as follows:

$$cS_{1,k} = \frac{2}{g_k}$$

This article has been accepted for inclusion in a future issue of this journal. Content is final as presented, with the exception of pagination.

$$F_k(s) = \frac{2D_k(s) - cS_{1,k}S_k(s)}{2}$$
$$E_k(s) = \frac{2D_k(s) + cS_{1,k}S_k(s)}{2}. \quad (23)$$

At this point, polynomial $P_k(s)$ is known to have the same roots as $P_k^{(0)}(s)$, and only its normalization constant remains to be computed by isolating it from (10). Notice that all the new contributions of $y_{in,k}$ have been computed, but there is still an L_{MUX} term if a shunt inductor is considered at the multiplexer common port. Going back to (9), observe that a fundamental condition must be fulfilled to ensure the monicity of the polynomial $S(s)$

$$L_{MUX} = \frac{1}{cD_3 \sum_{k=1}^{K} g_k - cS_2 - \sum_{k=1}^{K} g_k\, cX_{3,k}} \quad (24)$$

where cD_3 is the third highest degree coefficient of $D(s)$, cS_2 is the second highest degree coefficient of $S(s)$, and $cX_{3,k}$ is the third highest degree coefficient of product $X_k(s) = D_k(s)W_k(s)$.

Once the distorted channel polynomials are computed, the synthesis of each prototype filter is carried out separately. The extraction of the equivalent BVD elements of the AW resonator from a predefined filtering response can be achieved through the method described in [13], which is based on iterative evaluations of the input admittance. In this sequential extracted-pole process, each TZ is annihilated in turn and assigned to a specific resonator, so the TZ sorting is thus a degree of freedom at the extraction stage and does not affect the convergence of the iterative procedure. Following the same root-based philosophy described in Section IV, the admittance function can be updated without losing accuracy. Finally, the DB extracted elements are denormalized with a lowpass-to-lowpass frequency transformation ($\Omega = \omega/\omega_c$, where $\omega_c = 2\pi f_H$) because a dual-band symmetric about zero already exists.

E. Comprehensive Synthesis Steps

To enhance clarity, the complete DB synthesis algorithm proposed in this section can be summarized as follows.

1) *Step 1:* Given the channel settings (inner band limits, order, set of TZs and RL level), synthesize the LP of each filter by adding a complex RZ through RC functions. Then, map the single-band polynomials into the normalized real frequency domain, as detailed in Section III-A, to obtain $P_k^{(0)}(s)$, $F_k^{(0)}(s)$ and $E_k^{(0)}(s)$.
2) *Step 2:* Assemble polynomial $U(s)$ with $F_k^{(0)}(s)$ roots, considering only 1 of the K positive real RZs. Then, initialize $S_k^{(0)}(s)$ and $g_k^{(0)}$ from $F_k^{(0)}(s)$ and $E_k^{(0)}(s)$. If L_{MUX} is considered, $U(s)$ and $T_k(s)$ must be redefined as explained in Section III-B. Let $m = 0$.
3) *Step 3:* Build $T_k^{(m)}(s)$ and evaluate coefficients $|t_k^{(m)}|^2$ by imposing RL at one corner frequency per channel ($\Omega_{c,k}$).
4) *Step 4:* Compute $D^{(m)}(s)$ by solving FE.
5) *Step 5:* Update $S(s)$ and g_k from $D^{(m)}(s)$ and $U(s)$. Then, obtain the new estimation $S_k^{(m+1)}(s)$ by reordering the $S^{(m+1)}(s)$ roots such that the variance of their displacement with respect to the $S^{(m)}(s)$ roots is minimized.
6) *Step 6:* Set $m = m + 1$ and return to *Step 3* if a predefined criteria of convergence is exceeded. Reallocate common port RZ when $m = 1$, if required, and obtain a new version of $U(s)$ by the Remez-like procedure proposed in Section III-C. Otherwise, proceed to *Step 7*.
7) *Step 7:* Derive distorted channel polynomials and the junction inductor, if considered, following the procedure explained in Section III-D.

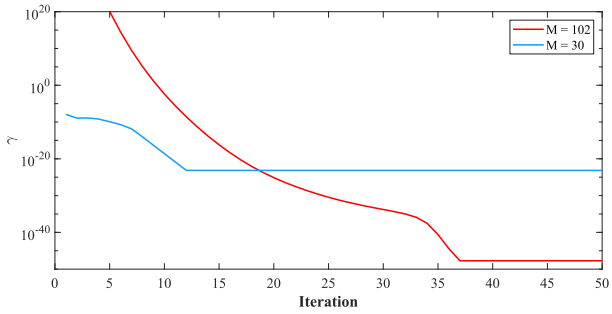

Fig. 7. Convergence evolution of the DK method by solving FE for $M = 30$ and $M = 102$, where the number of iterations needed to reach stable convergence values increases with polynomial order.

IV. Enhancing Numerical Stability of the Method

Beyond the synthesis framework, interpolation-based methods have shown numerical limitations when computing multiport polynomials during the iterative process. These include a restriction on handling high-order transfer functions and challenges in synthesizing narrow bands. This section focuses on enhancing numerical accuracy for polynomial evaluations and root-finding procedures, including the solution of the FE, whose formulation doubles the polynomial degree. Nevertheless, the practical order limit reported in [13] still applies to each individual channel, as it originates from the standalone RC filter synthesis prior to the bandpass mapping (i.e., $N_k \leq 18$ AW resonators).

A. Accurate Polynomial Representation

In general, polynomials are described by their coefficients. However, high-order polynomial interpolation often leads to significant round-off errors, primarily due to the extremely small values that appear in their last coefficients. As discussed in [17], to mitigate this issue, polynomials must be represented by their roots along with the leading coefficient, rather than by their full set of coefficients. For instance, the polynomial $U(s)$ is represented and computed as follows:

$$U(s) = u_0 \prod_{n=1}^{M} (s - zU_n). \quad (25)$$

Representing the polynomial in this way helps mitigate round-off errors in its evaluation, with the benefits becoming particularly significant when the roots are tightly spaced. Furthermore, the factorization-based strategy reduces numerical sensitivity and facilitates the use of numerical root-finding methods with enhanced precision.

This article has been accepted for inclusion in a future issue of this journal. Content is final as presented, with the exception of pagination.

B. Accurate Root-Finding Method

For the DB synthesis of multiplexers, numerical errors can significantly affect the computation of characteristic polynomials, as the coefficient values increase with filter order. As discussed in [17], the Durand–Kerner (DK) algorithm offers a reliable method to find polynomial roots, especially when addressing the double-degree FE. Despite these improvements, the convergence threshold (denoted as γ) in the DK algorithm remains highly sensitive to the polynomial order. Therefore, as the number of roots increases, a smaller threshold is required to ensure numerical stability. To illustrate this behavior, Fig. 7 shows the convergence evolution of the Feldtkeller solution for different multiplexer orders. This dependence translates into longer execution times for each synthesis iteration. Moreover, any pair of roots must fulfill the requirement of being neither equal nor symmetric about the imaginary axis. To further improve performance, a general eigenvalue-based vector fitting (VF) method is formulated for the first time in this work.

Let us consider that an arbitrary monic polynomial is expressed as

$$X(s) = \sum_{i=1}^{P} n_i N_i(s) \tag{26}$$

where P is the number of polynomials in the equation and n_i is the highest degree coefficient of $N_i(s)$.

While introducing a common denominator $Q(s)$ to both sides of (26) does not change the essence of the equation, it affects the way of pole identification significantly and thus can help improve the accuracy if $Q(s)$ is properly chosen. Therefore, now we can compute the i-term of the N-order polynomial in a partial fraction expansion format

$$\frac{N_i(s)}{Q(s)} = K_i + \sum_{k=1}^{N} \frac{r_{i,k}}{s - \lambda_k}. \tag{27}$$

This step involves the computation of the constant term K_i and residues $r_{i,k}$ [note that λ_k are directly the roots of $Q(s)$]. On the one hand, if both $N_i(s)$ and $Q(s)$ are monic polynomials and of the same order, the constant K_i corresponds to the leading coefficient n_i. On the other hand, residues $r_{i,k}$ can be derived as follows:

$$r_{i,k} = \frac{\prod_{l=1}^{N} (\lambda_k - zN_{i,l})}{\prod_{\substack{l=1 \\ l \neq k}}^{N} (\lambda_k - \lambda_l)}. \tag{28}$$

After considerations in (26) and (27), we can see that the unknown polynomial $X(s)$ can be also expressed as

$$\frac{X(s)}{Q(s)} = K_T + \sum_{k=1}^{N} \frac{c_k}{s - \lambda_k} \tag{29}$$

where

$$K_T = \sum_{i=1}^{P} K_i \quad c_k = \sum_{i=1}^{P} r_{i,k}. \tag{30}$$

Then, the zeros of the partial fraction expansion on the right-hand side of (29) can be directly computed as the eigenvalues of the matrix $(\mathbf{A} - K_T^{-1}\mathbf{BC})$ [27], where $\mathbf{A}$ is a diagonal matrix formed by the poles λ_k, $\mathbf{B}$ represents an all-one column vector, and $\mathbf{C}$ is a row vector of residues c_k.

Once an initial estimate of the roots of $X(s)$ has been obtained, it is recommended to relocate the poles λ_k (i.e., $Q(s)$ roots) through an iterative procedure. In particular, at the nth iteration polynomial $Q(s) = X^{(n)}(s)$, and the eigenvalue-based procedure is repeated. This iterative process continues until convergence is achieved. As a convergence criterion, the norm of the residue vector $\mathbf{C}$ can be evaluated. When the procedure converges, all elements of $\mathbf{C}$ should approach zero, indicating that the current poles are stable and the polynomial equation is accurately satisfied. Unlike the DK method, the VF method places no restrictions on pole allocation and quickly converges (typically, two and three iterations) under a norm criterion. Furthermore, this strategy can be extended for accurately solving the FE as discussed in [16].

C. Accurate Identification of $D_k(s)$ Roots

This section illustrates the modified NR method, originally developed in this work for the multiport DB synthesis framework, which is tailored to address the accurate identification of $D_k(s)$ roots. The NR method is a fast iterative numerical technique for finding the roots of a real function [28]. The extraction of the roots of the target polynomial is formulated as a nonlinear multivariable problem, where the unknowns are directly the roots rather than the polynomial coefficients. For our case, a system of $L = N_k^{DB} - 1$ nonlinear equations is solved by linearizing the problem around an initial guess and iteratively refining the solution. Given a vector function $\mathbf{f}(\mathbf{x})$, the update rule is given by

$$\mathbf{x}^{(t+1)} = \mathbf{x}^{(t)} - \mathbf{J}^{-1}\left(\mathbf{x}^{(t)}\right) \mathbf{f}\left(\mathbf{x}^{(t)}\right) \tag{31}$$

where $\mathbf{J}$ is the Jacobian matrix.

In this work, as commented before, $D_k(s)$ always has a root located at 0, so the unknowns are the remaining roots of this polynomial. For the kth channel, the reduced polynomial is expressed in factored form as

$$\tilde{D}_k(s) = \frac{D_k(s)}{s} = \prod_{i=1}^{L} \left(s - zD_{k,i}\right) \tag{32}$$

where $zD_{k,i}$ are the unknown roots to be determined.

The nonlinear system is constructed by evaluating a residual function $f(s)$ at prescribed points $s = zS_{k,v}$, $v = 1, \ldots, L$, where f_v follows the next expression:

$$f_v = \frac{G\, D\left(zS_{k,v}\right)}{C g_k W_k\left(zS_{k,v}\right)} - \tilde{D}_k\left(zS_{k,v}\right). \tag{33}$$

Unlike standard approaches where the polynomial is evaluated in terms of s, here the variables are the roots themselves. Therefore, the polynomial must be interpreted as the product of its roots, which inherently couples all variables. The solution is obtained iteratively using the modified NR method. At each iteration m, the roots are updated according to

$$zD_{k,i}^{(t+1)} = zD_{k,i}^{(t)} - \frac{f_v}{\dfrac{\partial f_v}{\partial zD_{k,i}}} \tag{34}$$

or, equivalently, in vector form

$$\mathbf{zD}_k^{(t+1)} = \mathbf{zD}_k^{(t)} - \mathbf{J}^{-1}\left(\mathbf{zD}_k^{(t)}\right) \mathbf{f}\left(\mathbf{zD}_k^{(t)}\right). \tag{35}$$

This article has been accepted for inclusion in a future issue of this journal. Content is final as presented, with the exception of pagination.

Interestingly, the derivatives of Jacobian matrix entries can be computed analytically as

$$J_{v,i} = \frac{\partial f_v}{\partial z D_{k,i}} = \prod_{j=1, j\neq i}^{L} \left(z S_{k,v} - z D_{k,j}\right). \tag{36}$$

The iterative process is repeated until a stable value for f_v is obtained, where convergence is assumed when $\max |\Delta f_v / f_v| < \delta$ (criteria of convergence δ typically set to $1e^{-3}$). Overall, this formulation enables the simultaneous update of all roots while accounting for their mutual interaction, leading to an efficient and robust reconstruction of the subpolynomials $D_k(s)$.

V. Synthesis Examples

This section presents two numerical examples to illustrate the capabilities of the proposed methodology in the context of star junction multiplexer synthesis. The first example provides a clear illustration of the algorithm presented in Section III, whereas the second example highlights its practical application in guiding AW multiplexer design. It is important to note that the synthesis stage maps the desired electrical response to the network parameters; manufacturing constraints such as resonator uniformity or finite coupling ranges belong to a subsequent design-optimization stage and do not affect the validity of the synthesis itself.

A. Duplexer With I/O Capacitors

In this section, a multiplexer example composed of two wideband ladder filters with a small guard bandwidth is presented with the purpose of assessing both the exact solution of the lossless reactive model and the numerical stability of the proposed DB methodology. The first channel operates in the $[400-650]$ MHz band and the second channel in the $[675-925]$ MHz band, giving an overall FBW of approximately 86.3%. For both channels, the imposed RL level is equal to 20 dB and composed of an 11th-order AW ladder filter starting in series resonator with the corresponding I/O capacitors. The chosen configuration includes the following normalized TZs and OoB RZs of each channel before the mapping in the DB domain.

1) *TZs (Ω):* [2.30, −2.02, 1.90, −1.92, 1.91, −1.90, 1.86, −1.92, 2.01, −1.98, 1.90], [2.10, −1.96, 2.00, −1.90, 1.93, −1.98, 1.95, −1.98, 1.97, −2.01, 2.06].
2) *Complex RZs (Ω):* $[6.47j]$, $[9.97j]$.

Note that, as described in [13], the imaginary part of Ω_{rz} corresponding to I/O capacitors is fixed to ensure symmetry with respect to the origin after the frequency mapping. Furthermore, the values of Ω_{rz} have been strategically selected to nullify the equivalent merged capacitance appearing at the common input node. This demonstrates that the additional degree of freedom introduced by the OoB RZs can be exploited to obtain solutions in which no external input reactive elements are required. After this consideration, the characteristic polynomials of the RC channel function are synthesized using the method in [24]. To obtain the DB filtering function of each channel, first the logarithmic mapping function described in (11) is used. After that, the dual-band roots must be mapped again into the overall $[-1, -f_L/f_H, f_L/f_H, 1]$ range of Ω that describes the multiplexer in the bandpass domain. As a result, the initial zeros of $P_k^{(0)}$ and $F_k^{(0)}$ are defined as follows:

$$\begin{aligned}
\Omega''_{\text{tz},1} &= [\,0.964, -0.964,\ 0.338, -0.338,\ 0.874, -0.874,\ 0.346, -0.346\\
&\quad 0.877, -0.877,\ 0.347, -0.347,\ 0.865, -0.865,\ 0.346, -0.346\\
&\quad 0.898, -0.898,\ 0.341, -0.341,\ 0.874, -0.874,\ 0]\\
\Omega''_{\text{tz},2} &= [\,1.190, -1.190,\ 0.627, -0.627,\ 1.171, -1.171,\ 0.633, -0.633\\
&\quad 1.159, -1.159,\ 0.625, -0.625,\ 1.161, -1.161,\ 0.625, -0.625\\
&\quad 1.166, -1.166,\ 0.622, -0.622,\ 1.182, -1.182,\ 0]\\
\Omega''_{\text{rz},1} &= [\,0.433, -0.433,\ 0.440, -0.440,\ 0.456, -0.456,\ 0.481, -0.481\\
&\quad 0.702, -0.702,\ 0.692, -0.692,\ 0.673, -0.673,\ 0.643, -0.643\\
&\quad 0.603, -0.603,\ 0.516, -0.516,\ 0.559, -0.559,\ \mathbf{j0.551},\ -\mathbf{j0.551}]\\
\Omega''_{\text{rz},2} &= [\,0.731, -0.731,\ 0.738, -0.738,\ 0.755, -0.755,\ 0.781, -0.781\\
&\quad 0.999, -0.999,\ 0.990, -0.990,\ 0.972, -0.972,\ 0.943, -0.943\\
&\quad 0.905, -0.905,\ 0.818, -0.818,\ 0.861, -0.861,\ \mathbf{j0.855},\ -\mathbf{j0.855}].
\end{aligned}$$

It can be observed that each channel includes a pair of purely imaginary RZs, but only one of the K associated with the input capacitor will be considered in the polynomial $U(s)$ (e.g., by taking the mean of RZs that must be merged into a single one). With the data provided so far, the iterative procedure described in Section III-B can now be initialized. After four iterations of the algorithm, the multiport polynomials are completely computed, and Fig. 8(b) shows the response of the obtained multiport polynomials in the DB domain. For comparison, Fig. 8(a) reports the multiport response of the same duplexer when the FE is solved through a coefficient-based representation instead of the root-based strategy, where the resulting numerical instability becomes apparent.

Then, the distorted channel polynomials $E_k(s)$, $P_k(s)$, and $F_k(s)$ along with normalization constants ε_k and $\varepsilon_{r,k}$ can be derived from the characteristic polynomials of the multiport function (whose coefficients/roots are not displayed due to a lack of space). Applying the methodology outlined in Section III-D, each channel filter defined with the DB approach is synthesized as a two-port network using the extraction methodology explained in [13].

After frequency scaling (i.e., $f_c = 925$ MHz), the BVD elements that compose each ladder network can be obtained. The

TABLE I
BVD Elements of the Duplexer Numerical Example

	Channel 1			Channel 2		
Resonator	L_a (nH)	C_a (pF)	C_0 (pF)	L_a (nH)	C_a (pF)	C_0 (pF)
1 (SE)	20.80	7.05	1.95	37.64	1.02	1.22
2 (SH)	14.03	18.52	13.05	10.89	6.92	8.47
3 (SE)	46.53	2.11	1.38	50.64	0.81	0.90
4 (SH)	12.02	20.57	13.53	10.10	7.31	9.06
5 (SE)	48.32	2.02	1.31	52.99	0.77	0.91
6 (SH)	11.94	20.54	13.56	9.15	8.29	9.53
7 (SE)	47.96	2.03	1.39	53.35	0.76	9.39
8 (SH)	12.05	20.49	13.47	9.34	8.11	9.39
9 (SE)	46.38	2.13	1.26	50.76	0.80	0.92
10 (SH)	14.83	17.16	12.02	11.72	6.53	8.27
11 (SE)	17.99	7.31	3.05	17.56	2.92	2.05
C_{out} (pF)		2.04			1.32	
Z_L (Ω)		47			51	

This article has been accepted for inclusion in a future issue of this journal. Content is final as presented, with the exception of pagination.

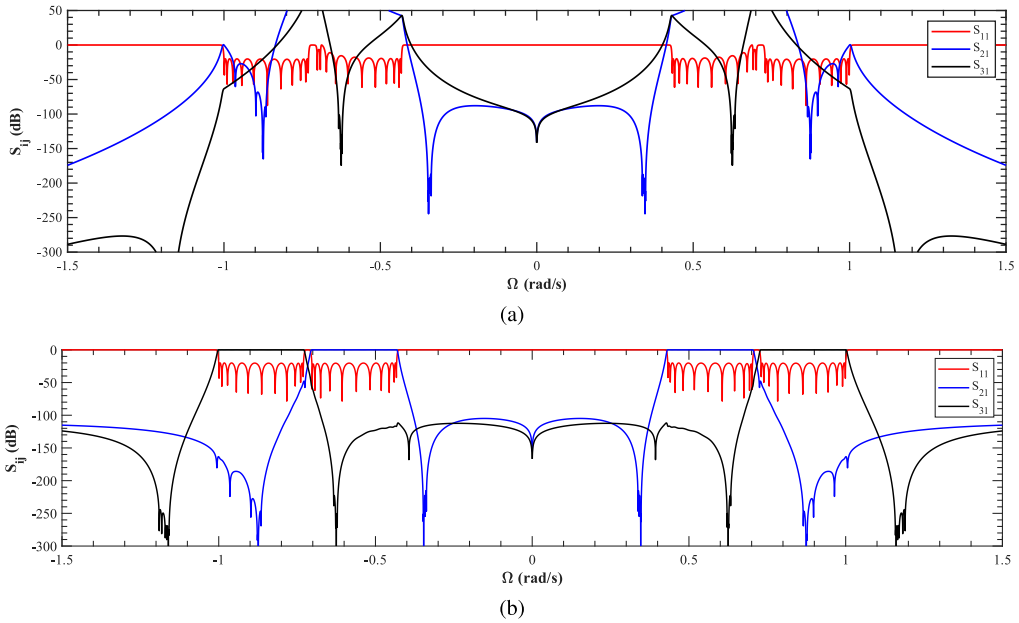

Fig. 8. Multiport transfer function response in the normalized domain of the duplexer using the computed DB multiport polynomials. (a) Solving the FE with a coefficient-based representation and (b) using the proposed root-based strategy.

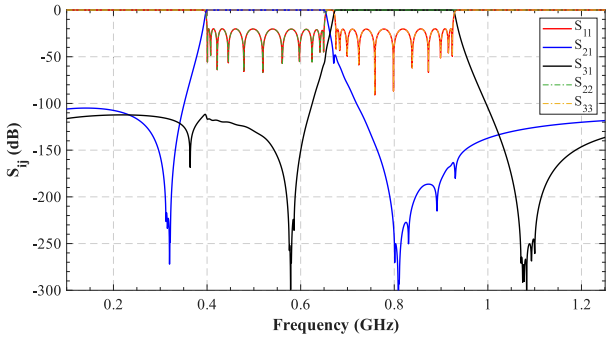

Fig. 9. Simulated response of extracted BVD parameters from synthesized duplexer with 11 AW resonators in each ladder filter.

resulting bandpass elements of the duplexer are summarized in Table I, where all filters start with a series (SE) resonator and include a shunt inductor at the I/O ports. Although the synthesized channel load impedances Z_L differ slightly from 50 Ω due to the asymmetric ladder synthesis, a final admittance redistribution could be applied without affecting the filter response. In addition, for this example, the input merged capacitor can be neglected. With the BVD elements, the simulated bandpass response of the multiplexer is shown in Fig. 9, depicting a practically CPRL equiripple of 20 dB for an antenna impedance of 50 Ω. Note that the reflection coefficients at the channel ports (S_{22} and S_{33}) are also included. Employing the ladder topology for implementing the channel filters, the circuit response computed from the reactance model perfectly aligns with the one computed from the multiplexer polynomials.

B. Quadplexer With Input Lc Tank and Output Capacitors

This example presents the complete synthesis procedure of an LTE Band 3 (1710–1785-MHz uplink and 1805–1880-MHz downlink) and Band 1 (1920–1980-MHz uplink and 2110–2170-MHz downlink) quadplexer to demonstrate the validity of the proposed method. The assumed requirements are seventh-order channels and a minimum CPRL of 14 dB. To provide a comparative analysis, we conduct two experiments employing the narrowband synthesis method discussed in [9] and the broadband synthesis method proposed in this article. Note that the method allows us to freely set the RL, TZs, and CRZ of each channel, enabling the search for multiplexers that fulfill the technological requirements of AW technology. Here are the LP synthesis input parameters of the four channels before the mapping in the DB domain.

1) *RL (dB):* 16.9, 14.3, 17.7, 17.7.
2) *TZs (Ω):* [1.85, −1.83, 1.69, −1.71, 1.70, −1.91, 1.28], [2.09, −1.86, 1.78, −1.80, 1.78, −1.94, 1.30], [2.62, −2.36, 2.27, −2.30, 2.27, −2.46, 1.25], [1.95, −1.89, 1.74, −1.76, 1.75, −1.96, 1.26].
3) *RZs for I/O Capacitors (Ω):* $10+73j$, $10+77j$, $10+99j$, $10+75j$.

For this second example, a shunt inductor is included at the common port of the multiport network in parallel with the merged input capacitor, both fixed by the conjugate pair of complex RZs Ω_{crz} = [−0.8500-0.2j, 0.85-0.2j]. This decision has been taken with the aim of adding a degree of freedom that helps to find a technologically feasible solution. As discussed in Section II-B, the inductor L_{MUX} will inherently affect the definition of the multiplexer transfer function. After applying the multiport iterative procedure, the characteristic polynomials of the multiplexer are completely synthesized using the proposed DB approach. Then, the distorted channel polynomials are derived, and the BVD parameters for the resonators forming each ladder filter are obtained. The resulting bandpass elements of the quadplexer are summarized in Table II. All filters include a shunt capacitor at the I/O ports (input capacitors merged into C_{MUX}) and a common port shunt inductor L_{MUX}, where for this solution the output capacitors of the first and last channels are negligible. This quadplexer

This article has been accepted for inclusion in a future issue of this journal. Content is final as presented, with the exception of pagination.

TABLE II
BVD ELEMENTS OF THE B3/B1 QUADPLEXER DB EXAMPLE

Multiplexer input elements				
$L_{MUX} = 2.45$nH		$C_{MUX} = 0.25$pF		
Band 3 uplink			$C_{out} = -$	$Z_L = 49.89\,\Omega$
Resonator	L_a (nH)	C_a (fF)	C_0 (pF)	k_t^2 (%)
1 (SE)	118.74	69.40	0.92	8.50
2 (SH)	28.84	311.31	4.13	8.50
3 (SE)	160.81	51.60	0.68	8.50
4 (SH)	27.82	321.10	4.26	8.50
5 (SE)	162.98	50.89	0.68	8.50
6 (SH)	30.85	292.07	3.87	8.50
7 (SE)	20.64	413.11	4.83	9.45
Band 3 downlink			$C_{out} = 0.27\,$pF	$Z_L = 48.06\,\Omega$
Resonator	L_a (nH)	C_a (fF)	C_0 (pF)	k_t^2 (%)
1 (SE)	143.78	51.26	0.68	8.50
2 (SH)	22.96	350.73	4.65	8.50
3 (SE)	153.66	48.57	0.64	8.50
4 (SH)	22.30	360.20	4.78	8.50
5 (SE)	154.64	48.26	0.64	8.50
6 (SH)	25.23	320.21	4.25	8.50
7 (SE)	24.53	311.35	3.94	8.87
Band 1 uplink			$C_{out} = 0.27\,$pF	$Z_L = 47.97\,\Omega$
Resonator	L_a (nH)	C_a (fF)	C_0 (pF)	k_t^2 (%)
1 (SE)	151.63	43.43	0.58	8.50
2 (SH)	15.67	457.87	6.07	8.50
3 (SE)	189.84	35.07	0.47	8.50
4 (SH)	14.63	489.68	6.50	8.50
5 (SE)	189.60	35.13	0.47	8.50
6 (SH)	17.91	401.80	5.33	8.50
7 (SE)	11.67	593.86	7.10	9.35
Band 1 downlink			$C_{out} = -$	$Z_L = 49.00\,\Omega$
Resonator	L_a (nH)	C_a (fF)	C_0 (pF)	k_t^2 (%)
1 (SE)	92.22	58.64	0.78	8.50
2 (SH)	21.79	271.06	3.60	8.50
3 (SE)	132.09	41.31	0.55	8.50
4 (SH)	20.99	279.93	3.71	8.50
5 (SE)	133.75	40.78	0.54	8.49
6 (SH)	23.77	249.12	3.31	8.48
7 (SE)	16.12	347.35	4.26	9.12

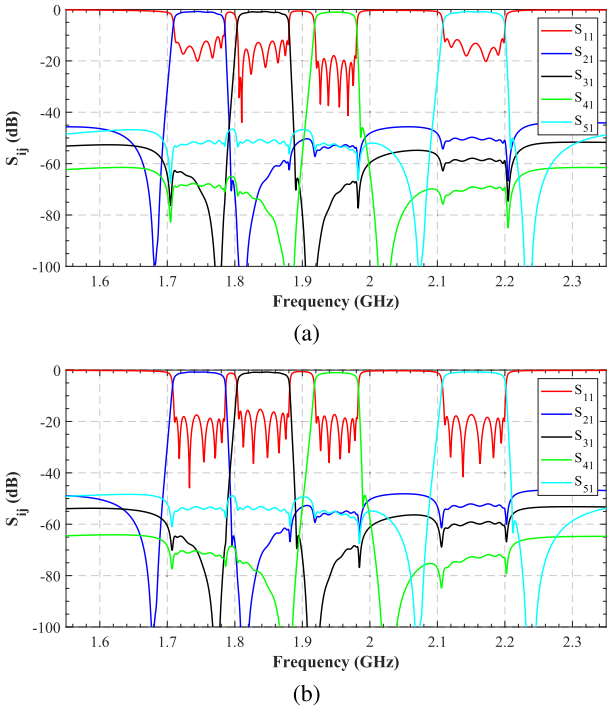

Fig. 10. Simulated response of the synthesized quadplexer using the mBVD model obtained by (a) narrowband approximation from [12] and (b) proposed broadband method.

TABLE III
COMPARISON OF NUMERICAL PERFORMANCE

Method	**Conv. Rates** $\Delta S^{(m)}$	**NR Iter.**	**Synth. Run**
[12]	$0.210^{(1)}$ $0.012^{(2)}$ $0.002^{(3)}$ $5.3\times10^{-5\,(4)}$	$t = 0$	~0.053 s
This work	$0.016^{(1)}$ $0.002^{(2)}$ $1.0\times10^{-4\,(3)}$ $1.7\times10^{-6\,(4)}$	$t = 15$ per k-channel	~0.189 s

example has been synthesized trying to be feasible using BAW resonators made of aluminum nitride (AlN) technology codoped with (Mg, Zr) [5], exhibiting $k_t^2 = 8.5\%$.

In parallel, the last quadplexer example using the same RL level and set of TZs of each channel in the LP domain is synthesized with the conventional narrowband technique. This alternative approach will result in different elements for the multiport network compared to those obtained with the proposed methodology. Furthermore, the simulated response of both synthesized multiplexers has been obtained using the modified BVD model (mBVD) presented in [29], and assuming an AW quality factor $Q_{AW} = 1500$, capacitor and inductor quality factors $Q_C = 150$ and $Q_L = 30$, respectively, and electrode resistivity $R_s = 0.25\ \Omega$.

Considering an antenna impedance of 50 Ω in both tests, Fig. 10(a) shows some degradation in the denormalized response due to the frequency transformation errors, mainly observed in the in-band matching of the filters (i.e., RL). Actually, the most significant contribution to the distortion in a wideband bandpass response comes from the frequency-dependent behavior of synthesized I/O FIRs, which are introduced at each individual channel filter to allow the correct extraction of ladder elements using narrowband techniques. On the contrary, a very good agreement between the synthesis and simulation of extracted network elements is depicted in Fig. 10 when the proposed method is used.

Beyond the response accuracy, the numerical behavior of the iterative procedure is assessed in Table III, comparing the proposed method against the narrowband synthesis of [12]. Three metrics are reported, averaged over several executions: the convergence rate of the multiport iterative procedure evaluated through the criterion $\Delta S^{(m)} = \max|(zS^{(m+1)} - zS^{(m)})/zS^{(m)}|$; the number of NR iterations required for the root identification of polynomials $D_k(s)$; and the execution time of a single synthesis run. Although the proposed method is slower than [12] due to the introduced NR loops, the convergence rate decreases monotonically to a stable value.

This article has been accepted for inclusion in a future issue of this journal. Content is final as presented, with the exception of pagination.

VI. Conclusion

This article proposes a novel DB synthesis methodology for AW multiplexers, addressing the limitations of conventional narrowband approaches. By reformulating the transfer function directly in the bandpass domain and explicitly modeling the asymptotic behavior at both the origin and infinity, the proposed method effectively mitigates frequency denormalization errors. It is evident that the proposed method requires a lot of numerical precision, but this limitation can be managed through refined polynomial evaluation and root-finding techniques. Also, it should be noted that the present formulation is not intended for the synthesis of contiguous multiplexers, where the proximity between channel passbands introduces additional challenges that will be addressed in future extensions of the methodology. The effectiveness of this approach is validated through two synthesis examples. On the one hand, the first example shows the perfect representation of the multiplexer response in the bandpass domain and the numerical stability of the method, achieving up to order 11 per channel. On the other hand, the second example shows very accurate results that can be used as a starting point from which to proceed with further multiplexer design stages down to the layout level. The fact that a seed design can be analytically obtained ensures an acceleration of the entire design process since it allows us to rapidly obtain the circuit elements of a new multiplexer response in case any of the filter TZs or RL need to be modified at any stage of a design cycle.

References

[1] P. Warder and A. Link, "Golden age for filter design: Acoustic filter, duplexer, and multiplexer approaches," *IEEE Microw. Mag.*, vol. 16, no. 7, pp. 60–72, Jul. 2015.

[2] G. G. Fattinger et al., "Carrier aggregation and its challenges-or: The golden age for acoustic filters," in *IEEE MTT-S Int. Microw. Symp. Dig.*, May 2016, pp. 1–4.

[3] P. Bradley, J. Kim, S. Ye, P. Nikkel, S. Bader, and C. Feng, "12E-0 2X size and cost reduction of film bulk acoustic resonator (FBAR) chips with tungsten electrodes for PCS/GPS/800 MHz multiplexers," in *Proc. IEEE Ultrason. Symp.*, Oct. 2007, pp. 1144–1147.

[4] P. Zhao and K.-L. Wu, "An iterative and analytical approach to optimal synthesis of a multiplexer with a star-junction," *IEEE Trans. Microw. Theory Techn.*, vol. 62, no. 12, pp. 3362–3369, Dec. 2014.

[5] A. Hagelauer, G. Fattinger, C. C. W. Ruppel, M. Ueda, K.-Y. Hashimoto, and A. Tag, "Microwave acoustic wave devices: Recent advances on architectures, modeling, materials, and packaging," *IEEE Trans. Microw. Theory Techn.*, vol. 66, no. 10, pp. 4548–4562, Oct. 2018.

[6] C. C. W. Ruppel, "Acoustic wave filter technology—A review," *IEEE Trans. Ultrason., Ferroelectr., Freq., Control*, vol. 64, no. 9, pp. 1390–1400, Sep. 2017.

[7] A. Giménez, J. Verdú, and P. De Paco Sánchez, "General synthesis methodology for the design of acoustic wave ladder filters and duplexers," *IEEE Access*, vol. 6, pp. 47969–47979, 2018.

[8] E. Guerrero, P. Silveira, J. Verdú, Y. Yang, S. Gong, and P. de Paco, "A synthesis approach to acoustic wave ladder filters and duplexers starting with shunt resonator," *IEEE Trans. Microw. Theory Techn.*, vol. 69, no. 1, pp. 629–638, Jan. 2021.

[9] E. Guerrero, L. Acosta, J. Verdú, and P. de Paco, "Direct synthesis of acoustic wave multiplexers built on fully canonical multiport functions," *IEEE Trans. Microw. Theory Techn.*, vol. 71, no. 4, pp. 1391–1401, Apr. 2023.

[10] P. Silveira, J. Verdú, and P. de Paco, "Star-junction multiplexer design under minimum susceptance networks approach," in *IEEE MTT-S Int. Microw. Symp. Dig.*, Jun. 2019, pp. 1194–1197.

[11] S.-Y. Tseng, M.-Y. Yang, C.-C. Hsiao, Y.-Y. Chen, and R.-B. Wu, "Design for acoustic wave multiplexers with single inductor matching network using frequency response fitting method," *IEEE Open J. Ultrason., Ferroelectr., Freq. Control*, vol. 2, pp. 140–151, 2022.

[12] M. Faura, G. Reixach, L. Acosta, C. Caballero, J. Verdú, and P. De Paco, "Design of high-order acoustic wave manifold multiplexers using factorization-based strategy in multiport synthesis," *IEEE Access*, vol. 13, pp. 202539–202552, 2025.

[13] S. Cano, C. Caballero, O. Barrera, R. Lu, J. Verdú, and P. de Paco, "General synthesis methodology for acoustic wave ladder filters in the bandpass domain," *IEEE Trans. Microw. Theory Techn.*, vol. 73, no. 10, pp. 7055–7068, Oct. 2025.

[14] S. Cano, J. Verdú, and P. de Paco, "Coupling matrix decomposition of acoustic wave ladder filters in the bandpass domain," *IEEE Trans. Microw. Theory Techn.*, vol. 74, no. 1, pp. 569–580, Jan. 2026.

[15] Y. Wu, K. Yang, F. Lin, Y. Zeng, and M. Yu, "Acoustic wave filter synthesis: From characteristic polynomials to circuit models," *IEEE Trans. Microw. Theory Techn.*, vol. 74, no. 7, pp. 1–11, Jul. 2026.

[16] P. Zhao, B. Liu, M. Oldoni, and Y. Yang, "Improving accuracy in solving feldtkeller equation," *IEEE Microw. Wireless Technol. Lett.*, vol. 34, no. 3, pp. 251–254, Mar. 2024.

[17] B. Liu, G. Macchiarella, Y. Yang, Y. Zhang, and M. Yu, "Comprehensive analytical synthesis of star-junction multiplexers with guaranteed equiripple responses," *IEEE Trans. Microw. Theory Techn.*, vol. 73, no. 6, pp. 3285–3297, Jun. 2025.

[18] M. Faura, S. Cano, J. Mesas, L. Gracía, J. Verdú, and P. De Paco, "Broadband modeling of star junction acoustic wave multiplexers through synthesis methodology," in *Proc. IEEE Int. Microw. Filter Workshop (IMFW)*, Feb. 2026, pp. 1–3.

[19] T. Jamneala, P. Bradley, D. Feld, D. Clark, and A. Chien, "A generic passive matching network for multiplexers," *IEEE Trans. Ultrason., Ferroelectr., Freq. Control*, vol. 54, no. 6, pp. 1272–1275, Jun. 2007.

[20] R. J. Cameron, C. M. Kudsia, and R. R. Mansour, *Microwave Filters for Communication Systems*. Hoboken, NJ, USA: Wiley, Mar. 2018.

[21] R. Baum, "Design of unsymmetrical band-pass filters," *IRE Trans. Circuit Theory*, vol. 4, no. 2, pp. 33–40, 1957.

[22] G. Macchiarella and S. Tamiazzo, "Synthesis of star-junction multiplexers," *IEEE Trans. Microw. Theory Techn.*, vol. 58, no. 12, pp. 3732–3741, 2010.

[23] G. Macchiarella, "'Equi-ripple' synthesis of multiband prototype filters using a Remez-Like algorithm," *IEEE Microw. Wireless Compon. Lett.*, vol. 23, no. 5, pp. 231–233, May 2013.

[24] S. Tamiazzo, G. Macchiarella, and F. Seyfert, "Path filters: A class of true inline topologies with transmission zeros," *IEEE Trans. Microw. Theory Techn.*, vol. 70, no. 1, pp. 850–863, Jan. 2022.

[25] J. Verdú, M. Faura, L. Acosta, E. Guerrero, C. Caballero, and P. De Paco, "Synthesis of the double-ladder topology with arbitrary bandwidths and dual-band response," in *IEEE MTT-S Int. Microw. Symp. Dig.*, Jun. 2022, pp. 8–11.

[26] M. Faura, C. Caballero, J. Verdú, and P. de Paco, "Analytical improvement of common port return loss equiripple in multiport network synthesis," *IEEE Microw. Wireless Technol. Lett.*, vol. 35, no. 8, pp. 1106–1109, Aug. 2025.

[27] S. Grivet-Talocia and B. Gustavsen, *Passive Macromodeling: Theory and Applications*. Hoboken, NJ, USA: Wiley, 2015.

[28] R. L. Burden and J. D. Faires, *Numerical Analysis*, 9th ed., Pacific Grove, CA, USA: Brooks/Cole, 2011.

[29] J. D. Larson, P. D. Bradley, S. Wartenberg, and R. C. Ruby, "Modified Butterworth-Van Dyke circuit for FBAR resonators and automated measurement system," in *Proc. IEEE Ultrason. Symp.*, San Juan, PR, USA, Mar. 2000, pp. 863–868.

Mario Faura (Graduate Student Member, IEEE) was born in Barcelona, Spain, in 2000. He received the B.S. (Hons.) and M.S. degrees in telecommunications engineering from the Universitat Autónoma de Barcelona (UAB), Barcelona, in 2021 and 2023, respectively, where he is currently pursuing the Ph.D. degree at the WavesLab Group.

His main research interests include the synthesis of microwave filters and the synthesis and design of microwave acoustic filters and multiplexers.

This article has been accepted for inclusion in a future issue of this journal. Content is final as presented, with the exception of pagination.

Joel Mesas (Graduate Student Member, IEEE) was born in Barcelona, Spain, in 2001. He received the B.S. and M.S. degrees in telecommunications engineering from the Universitat Autónoma de Barcelona (UAB), Barcelona, in 2022 and 2024, respectively, where he is currently pursuing the Ph.D. degree at the WavesLab Group.

His main research interests include advanced synthesis methodologies for microwave and acoustic-wave filters for wireless applications, with particular emphasis on the systematic exploration of unconventional filter topologies through numerical reconfiguration techniques.

Santi Cano (Graduate Student Member, IEEE) was born in Sabadell, Spain, in 2000. He received the B.S. and M.S. degrees in telecommunications engineering from the Universitat Autónoma de Barcelona (UAB), Barcelona, Spain, in 2021 and 2023, respectively, where he is currently pursuing the Ph.D. degree at the WavesLab Group.

His main research interests include the synthesis of microwave filters and the synthesis and design of microwave acoustic filters for wireless communications applications.

Laia Garcia (Graduate Student Member, IEEE) was born in Granollers, Spain, in 2000. She received the B.S. and M.S. degrees in telecommunications engineering from the Universitat Autónoma de Barcelona (UAB), Barcelona, Spain, in 2021 and 2023, respectively, where she is currently pursuing the Ph.D. degree at the WavesLab Group.

Her main research interests include the identification of design deviations in microwave acoustic filters and their synthesis and design for wireless communication applications.

Jordi Verdú (Senior Member, IEEE) was born in Sabadell, Spain. He received the M.S. degree in telecommunication engineering and the Ph.D. degree (cum laude) from the Universitat Autónoma de Barcelona (UAB), Barcelona, Spain, in 2006 and 2010, respectively.

In 2010, he was a Group Coordinator with the RF System Group, European Spallation Source at Bilbao (ESS-B), Biscay, Spain. In 2011 and 2012, he was at the École Polytechnique Fédérale de Lausanne through a Marie Curie grant. In 2013, he was at the Theory Signal Communication Group, Universitat Politécnica de Catalunya, Barcelona. Currently, he is an Associate Professor at the Universitat Autónoma de Barcelona, where he teaches microwave engineering courses and is a member of the WavesLab Group. He has been extensively working on linear modeling of acoustic wave devices, and new synthesis techniques and advanced configurations for acoustic wave filters. His current research interests include the design of microwave devices, linear modeling, and the design of active devices for Space applications.

Dr. Verdú was a member of the Antenna and Microwave Systems (AMS) from 2006 to 2010. He is the Vice-Chair of the MTT-6 MEMS and Microwave Acoustics Technical Committee.

Pedro de Paco (Senior Member, IEEE) was born in Badalona, Spain. He received the M.S. degree in telecommunication engineering and the Ph.D. degree (cum laude) from the Universitat Politécnica de Catalunya (UPC), Barcelona, Spain, in 1997 and 2003, respectively.

In 1998, he joined the Electromagnetic and Photonics Engineering Group (EEF), Signal Theory and Communications Department (TSC), UPC, with a grant from the Institut d'Estudis Espacials de Catalunya (IEEC), Barcelona, in a joint activity related to the European Scientific Space Mission Planck, Noordwijk, The Netherlands. He was a member of the LFI-Radiometer Working Group and the Planck Consortium. During his Ph.D., he participated in several national and international research projects mostly related to microwave and millimeter-wave circuits and systems applied to the design and testing of remote sensing instruments and front-end-to-multipoint broadband communication systems. Since 2004, he has been an Associate Professor with the Universitat Autónoma de Barcelona (UAB), Barcelona, where he teaches applied electromagnetics and microwave engineering courses. From 2010 to 2013, he was the Deputy Director and a member of the Executive Board at the Department of Telecommunication and System Engineering, UAB. From 2018 to 2019, he was a Visiting Researcher with the Microwave and RF Research Group, University of Colorado Boulder, Boulder, CO, USA. He has advised eight Ph.D. students. His main research interests include microwave filter synthesis, microwave acoustics filter synthesis and design, and microwave and radar systems and devices.

Dr. de Paco is a member of the MTT-6 RF MEMS and Microwave Acoustics Committee. He was awarded three times with merits in research and recognized with merits at University training by l'Agéncia de Qualitat, and awarded with Advanced Research by Generalitat de Catalunya. He is a reviewer of IEEE TRANSACTIONS ON MICROWAVE THEORY AND TECHNIQUES and IEEE MICROWAVE AND WIRELESS COMPONENTS LETTERS. He serves as a member of the Technical Review Board for the European Microwave Conference. He has been appointed as a Technical Expert for Telecommunications Equipment by the National Agency of Accreditation.